Energetic particle events at traveling interplanetary shocks: modeling between 20 keV and 500 MeV

M.-B. Kallenrode[1] and R. Hatzky[2]
[1] Inst. f. Umweltkommunikation, Universität Lüneburg, Germany
[2] University of Kiel, Germany; now at MPI für Plasmaphysik, Greifswald, Germany

Abstract

We present an extension of an earlier black-box model to include the effects of adiabatic deceleration and convection with the solar wind in addition to pitch-angle scattering and focusing in the propagation of particles accelerated at an interplanetary shock. This model allows to infer the development of shock acceleration along the observer's magnetic field line together with the scattering mean free path from intensity and anisotropy time profiles.

1. Introduction

The acceleration of energetic particles at transient interplanetary shocks can be observed up to energies of about 100 MeV. While the acceleration process up to a few hundred keV is fairly well understood, the acceleration of MeV particles and its dependence on the shock's plasma parameter is less well understood. One attempt to gain insight into this problem is the use of a model which combines the shock as a black-box, described by an acceleration efficiency, and the subsequent transport of the accelerated particles through interplanetary space. Such a model allows to infer the development of the particle acceleration along the observer's magnetic field line and the radial scattering mean free path λ_r. Models were proposed by Heras et al. (1992) and Kallenrode and Wibberenz (1997, KW97), both based on the focused transport equation (Roelof, 1969), and by Lario et al. (1998) using an expanded version of the transport equation (Ruffolo 1995) which also considers the solar wind effects such as adiabatic deceleration and convection of particles with the solar wind. In this paper we expand the model by KW97 to include solar wind effects. The differences compared to the model by Lario et al. (1998) basically are the assumptions about the shock: we will start with rather simple assumptions while Lario et al. (1998) use MHD simulations of interplanetary shocks. The basic differences were already discussed in KW97 for the simpler models starting from the Roelof equation.

2. The Model

The transport equation used in this model has been proposed by Ruffolo (1995) and considers the effects of pitch-angle scattering, focusing in the diverging interplanetary magnetic field, convection with the solar wind, and adiabatic deceleration. We will here use the numerical code by Hatzky (1996), cf. Hatzky and Kallenrode (1999), complemented by a source which can vary not only in time but also in space, cf. KW97. This shock is specified as follows: (1) the shock is spherical symmetric and expands at a constant speed; although this is physically incorrect, in particular as the shock speed decreases towards the flanks and with increasing radial distance, the results are not strongly influenced by this assumption, cf. Fig.

6 in KW97. However, if we attempt to relate the inferred injection from the shock front to shock speed, this assumption has to be dropped and replaced by a more realistic motion of the cobpoint along the shock front.
(2) the acceleration efficiency depends on radial distance r and angular distance $\phi_{\rm con}(t)$ from the nose of the shock and is described by a separation ansatz

$$Q = Q_{\rm o} \cdot \left(\frac{r}{r_{\rm o}}\right)^{\alpha} \cdot \exp\left\{-\frac{\phi_{\rm con}(t)}{\phi_c}\right\} \ ,$$

with $\phi_{\rm c}$ being the e-folding angle of the intensity along the shock front. The injection is isotropic at the shock front, that is particles are injected into the upstream and downstream medium. In addition, a separate solar injection can be assumed, if necessary.
(3) additional turbulence upstream of the shock can be included (but not self-consistently).
(4) the background magnetic field is assumed to be Archimedian. Obviously, this is not valid in the downstream medium. However, variations with downstream focusing and downstream scattering show that the assumptions about the downstream medium do not strongly influence the results of the model, cf. Fig. 3 in KW97.
The relevant parameters to be specified in the model then are (1) the radial particle mean free path $\lambda_{\rm r}$ (in a more advanced version this depends on particle rigidity: $\lambda \sim P^{0.3}$), (2) the injection $S(r,\phi)$ from the shock front, and (3) a solar injection $S_\odot$, if required.

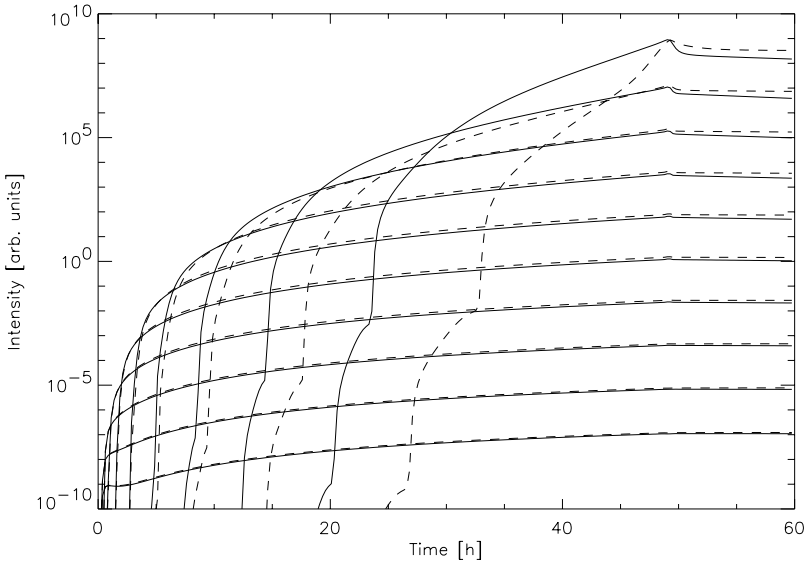

Fig. 1: Intensity time profiles with (solid) and without (dashed) solar wind effects for different energies (20, 66, 220, and 730 keV, 2.4, 8, 26, 85, 260, and 711 MeV), a radial mean free path $\lambda_{\rm r} = 0.1$ AU, a shock speed of 800 km/s, and constant acceleration efficiency along the observer's magnetic field line. The shock passes the observer at $t = 48$ h.

3. Results

Figure 1 shows a comparison of the results for the 'standard' shock of KW97 (shock speed 800 km/s, observer at a radial distance of 1 AU, particle mean free path $\lambda_{\rm r} = 0.1$ AU independent of particle speed, no turbulent upstream region, particle energies from 20 keV to 700 MeV, the injection from the shock is constant along the entire field line, its spectral index is -3.5) under consideration of solar wind effects (solid lines) and neglecting solar wind effects (dashed). As in the case of a solar injection, the consideration of solar wind effects leads to an earlier onset. This is most obvious in the lower energies where average particle speeds are comparable to the solar wind speed. Correspondingly, the intensity increase upstream of

the shock is much flatter than without consideration of solar wind effects. The typical faster decay of the intensity, however, is much less pronounced than in case of a solar injection (cf. Fig. 1 in Hatzky and Kallenrode, 1999): in particular in the higher energies this decay is predominately due to adiabatic deceleration. To become effective, this process takes time, the characteristic time constant at 1 AU is a few days. In case of the continuous injection of particles from the shock, always a fresh supply of particles is added on top of the previous injections. These later injections therefore suffer less from adiabatic deceleration. As a consequence, solar wind effects are of minor importance for energies in the MeV range or higher. This belately justifies the use of the more simple model by KW97 for fitting particle events observed in the MeV range (Kallenrode, 1997a,b). However, we should be aware that the above statement is made for a shock with constant acceleration efficiency along the observer's magnetic field line. If the acceleration efficiency increases, the same reasoning is true. In case of a decreasing acceleration efficiency, the situation is in between the solar injection and the situation depicted in Fig. 1, that is although solar wind effects become more prominent they still are less pronounced than for a solar injection, as can be seen from Fig. 2. Note that an increase in scattering conditions leads to more pronounced solar wind effects mainly for a shock acceleration efficiency decreasing along the observer's field line but does not enhance the differences in case of constant or increasing shock efficiency. In addition, solar wind effects will increase with increasing radial distances because of the longer time scales.

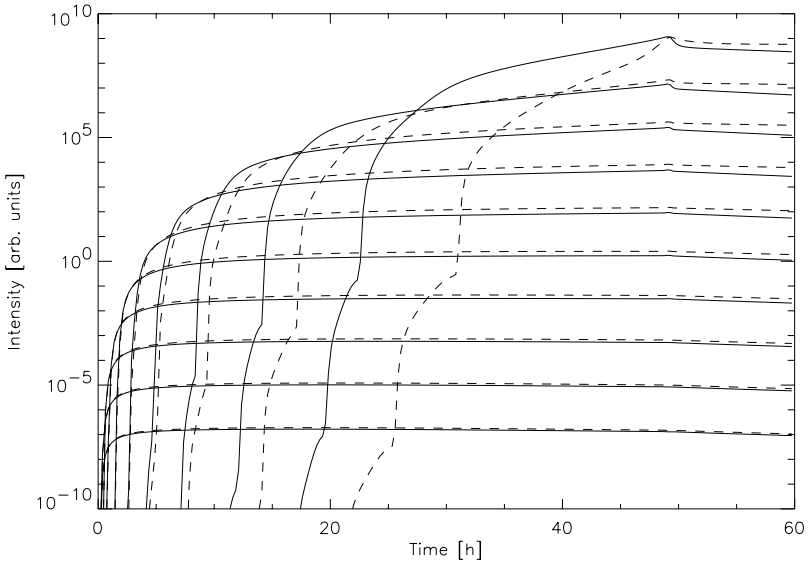

Fig. 2: same as Fig. 1 but the shock efficiency decreases as r^{-2} along the observer's magnetic field line.

Figure 3 shows 3 sets of intensity profiles for different locations of the observer relative to the nose of the shock. Again, shock speed is 800 km/s, the shock efficiency is assumed to not depend on radius ($\alpha = 0$) but only on azimuthal distance from the nose of the shock with a characteristic e-folding angle of 15°. These profiles reproduce the basic relations known from the observations: at the eastern flank of the shock, the intensity rises to an early maximum with the time of maximum decreasing with increasing particle energy and decreases towards the approaching shock while at the western flank the intensity continues to rise towards the shock, even in the higher energies. The differences between the different locations would be more pronounced if a smaller e-folding angle is chosen (as e.g. the 10° suggested in KW97). Note that in this model the profiles further to the east/west are similar to the E50/W25 profiles

except for the absolute intensity. This is a direct consequence of the separation ansatz.

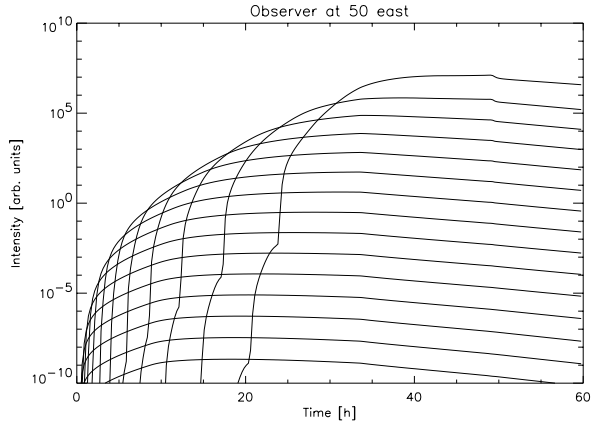

Fig. 3: Intensity time profiles for observer at different locations with respect to the nose of the shock: for an observer on the eastern flank of the shock, the intensity rises to an early maximum and decreases towards the shock while an observer on the western flank sees a continuous intensity increase towards the shock.

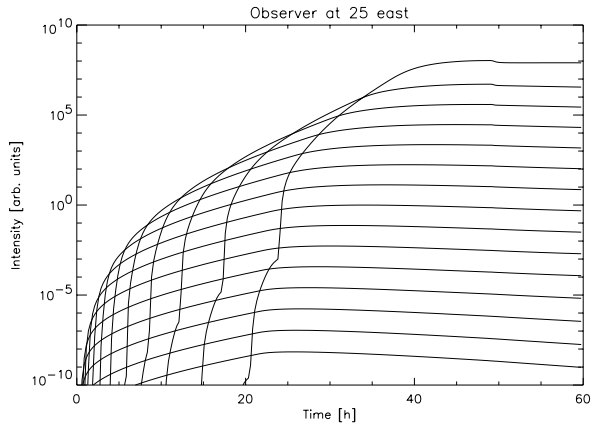

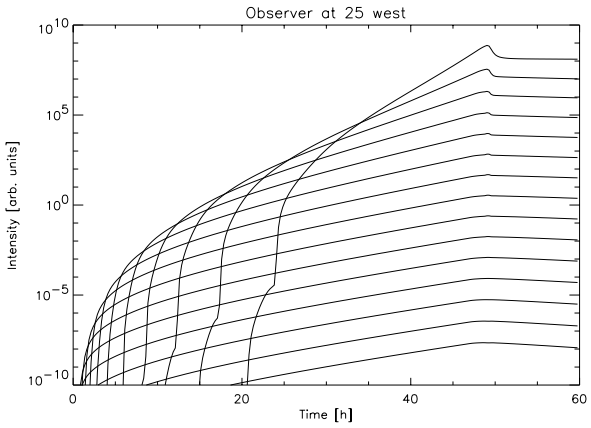

4. Conclusions

Our model shows that, as expected, solar wind effects influence the particle distributions at shock associated events in a similar manner as in solar energetic particle events, however, their influence is smaller, owing to the fact that the time lag between the injection and the observation is smaller because of the continuous injection.

Acknowledgments. This work was supported by the Deutsche Forschungsgemeinschaft under contract DFG Kal1297/1-3.

References

Hatzky, R., and M.-B. Kallenrode, *26th ICRC*, paper SH 1.6.07, this volume, 1999
Heras, A.M., B. Sanahuja, Z.K. Smith, T. Detman, and M. Dryer, *APJ 391*, 359, 1992
Kallenrode, M.-B., and G. Wibberenz, *JGR 102*, 22 311, 1997
Kallenrode, M.-B., *JGR 102*, 22 335, 1997
Kallenrode, M.-B., *JGR 102*, 22 345, 1997
Lario, D., B. Sanahuja, and A.M. Heras, *APJ 509*, 415, 1998
Roelof, E.C., in *Lectures in High Energy astrophysics* (eds. H. Ögelmann, J.R. Wayland), NASA SP-199, 111, 1969
Ruffolo, D., *APJ 442*, 861, 1995